Rare Metal Materials and Engineering
Volume 50, Issue 3, March 2021
Available online at www.rmme.ac.cn

Science Press

Cite this article as: Rare Metal Materials and Engineering, 2021, 50(3): 0802-0806.

ARTICLE

Improvements of Mechanical Properties of WC-ZrO_2 Composites with Addition of Ultrafine Porous Boron Nitride Nanofiber

Cao Ting[1], Li Xiaoqiang[1], Li Jingmao[1], Huang Yang[2], Song Tao[2], Qu Shengguan[1], Liang Liang[1]

[1] South China University of Technology, Guangzhou 510640, China; [2] Hebei University of Technology, Tianjin 300130, China

Abstract: An ultrafine porous boron nitride nanofiber was added to WC-8wt%ZrO_2 composite, aiming to improve the mechanical properties of composite. The results show that the Young's modulus, fracture toughness and hardness of the obtained composite specimens increase with the addition of the fiber. However, the increase of Young's modulus of the specimens does not follow the rule of mixtures for most ceramics-based composites. The tested value of several specimens after adding 0.05wt% porous boron nitride fiber is up to 692 GPa which is close to the Young's modulus of pure WC of 700 GPa. The phenomenon can be elucidated by small size effect of nanomaterials, based on the superplasticity of ZrO_2.

Key words: porous nanofibers; WC; ZrO_2; Young's modulus

WC-Co materials are generally used in cutting tools. In the last thirty years, because of the improved corrosion resistance, WC ceramics without binders were investigated as alternatives of WC-Co materials[1-3]. ZrO_2 is well known because of transformation property, which can be employed as toughening phase[4-6]. Moreover, WC-ZrO_2 composites were reported previously[7-9]. However, the ceramic/ceramic interface shows a weak bonding that is beneficial for toughening according to traditional toughening theory, which can subsequently lead to abrasive wear[8]. In this study, an ultrafine porous boron nitride nanofiber was introduced into a WC-8wt%ZrO_2 composite which shows the optimized mechanical properties reported in our previous work[9]. The fiber possesses high porosity and turbostratic structure with a high specific surface area of 515 $m^2 \cdot g^{-1}$ and a total pore volume of 0.566 $cm^3 \cdot g^{-1}$ [10]. Phenomena such as toughening under strong interface bonding without binders and enhancement of Young's modulus beyond the rule of mixtures were observed and discussed.

1 Experiment

Commercially available WC (200 nm, purity>99.9%, Xuzhou Jiechuang New Material Technology Co., Ltd, China), 3Y-ZrO_2 (~0.1 μm, 3 mol% Y_2O_3-stabilized tetragonal ZrO_2, 6.05 $g \cdot cm^{-3}$, Shanghai Chemson Chemical Co., Ltd, China), and UPBNNF (diameter: 20~60 nm; length: tens micrometers; Boron Nitride Research Center, Hebei University of Technology, China) were used as raw materials. WC-ZrO_2-UPBNNF powder mixtures with 0wt%, 0.05wt%, 0.1wt%, and 0.15wt% UPBNNF after the addition of 8wt% ZrO_2 were wet-mixed in a planetary ball mill (QM-3SP4, Nanjing Nanda Instrument Plant, China) with ethanol using cemented carbide milling balls (ball-to-powder mass ratio=4:1) and cemented carbide vials (250 mL). To minimize the potential Co contamination from the milling balls or vials, milling was performed through a low-energy mode: the milling process paused for 18 min after every 30 min milling cycle, restarted reversely at a constant rotation speed of 180

Received date: March 27, 2020
Foundation item: National Natural Science Foundation of China (51474108, 51575193, 51402086); Hundred Talents Program of Hebei Province (E2014100011); Key Project of Guangdong Natural Science Foundation (2018B030311051); Heyuan Science and Technology Project (heke2018009)
Corresponding author: Li Xiaoqiang, Professor, National Engineering Research Center of Near-Net-Shape Forming for Metallic Materials, South China University of Technology, Guangzhou 510640, P. R. China, Tel: 0086-20-87112111, E-mail: lixq@scut.edu.cn

r/min, and finally stopped after 60 cycles of milling. Furthermore, to eliminate the agglomerates which may lead to poor sinterability, the milled powders were dried and sieved. The obtained WC-UPBNNF powders were poured into a cylindrical graphite die with an inner diameter of 20 mm and an outer diameter of 50 mm. The sintering was performed on a Dr.Sinter Model SPS-825 SPS system (Sumitomo Coal Mining Co., Ltd, Japan) in vacuum (≤6 Pa) at a heating rate of 100 °C/min under the applied pressure of 30 MPa. All specimens were heated to 1600 °C holding for 5 min. During the sintering process, graphite paper was used to separate the powder from graphite die or punches, and then the die was surrounded with a porous carbon insulation belt to minimize the radiation heat loss. Furthermore, at the bottom of the central core hole in the die wall, i.e., 2.5 mm away from the inner wall, an infrared pyrometer (≥570 °C) was focused. The obtained WC-UPBNNF specimens were named as 8Z, 8Z0.05, 8Z0.1, and 8Z0.15 in terms of their UPBNNF content.

The density of the specimens was measured using water and calculated according to ASTM B311-13. The hardness (H) was evaluated on a Vickers hardness tester (430SVA, Wilson Wolpert Co., Ltd, China) with the load of 10 kg. The fracture toughness (K_{Ic}) was calculated based on the radial crack produced by Vickers indentation (HV_{10}) according to Niihara formula:

$$K_{IC} = 0.018Ha^{\frac{1}{2}}(\frac{E}{H})^{\frac{2}{5}}(\frac{c}{a}-1)^{\frac{1}{2}} \quad (1)$$

where E is Young's modulus, H is hardness, a is half-diagonal of the indent, and c is radius of the surface crack[11]. The values are the average of the data obtained from five indentation tests. Using the pulse-echo overlap ultrasonic technique, the elastic modulus of all samples was determined (examined in School of Materials Science & Engineering, Dalian University of Technology). Phase identification was conducted by an X-ray diffractometer (XRD, D8 Advance, Bruker Co., Ltd, Germany) with Cu Kα radiation. Finally, the microstructure and Vickers indentations were examined by a high-resolution scanning electron microscope (HRSEM, Nova Nano 430, FEI, USA) and scanning transmission electron microscope (STEM, JEM-2010, JEOL, Japan).

2 Results and Discussion

Fig.1 shows the densification curves of composite specimens which were heated to 1600 °C holding for 5 min. The densification process starts when the shrinkage rate turns to be positive after the vibration in early stage because of the thermal expansion of the compacted powders. The process continues until the shrinkage rate decreases to zero. For all specimens, the densification process is at the temperature of 850~1550 °C. As shown in Fig.1, UPBNNF addition does not obviously change the densification behavior of specimens. Density characteristics of composites are listed in Table 1, indicating that the composites containing UPBNNF has higher density.

Fig.2 shows the XRD patterns of composites. Owing to the small mass fraction of UPBNNF, the XRD patterns show the peaks of sintered WC and ZrO_2. There are no monoclinic ZrO_2 phase peaks in the patterns except for 8Z, which confirms the inhibiting effect of UPBNNF in the monoclinic phase. Fig.3 shows the microstructures of specimens comprising gray WC grains and dark ZrO_2 particles, which have not distinct difference from our previous WC-ZrO_2 study[8]. UPBNNF cannot be well-examined in the composites, especially in ZrO_2 composites. Therefore, UPBNNFs can only be observed in WC grains by STEM, as shown in Fig.4.

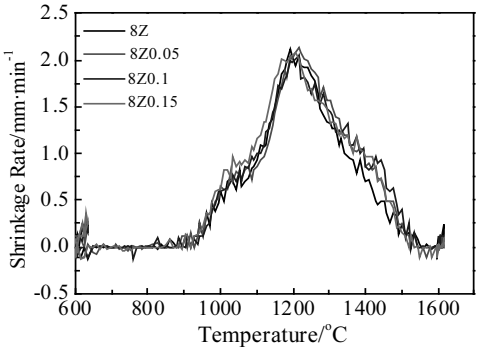

Fig.1 Densification curves of composite specimens

Table 1 Characteristics of composite specimens

Specimen	Density/ g·cm^{-3}	Hardness/ GPa	Fracture toughness/ MPa·m$^{1/2}$
8Z	13.67	23.15±0.63	8.59±0.86
8Z0.05	13.73	24.52±0.43	8.92±0.16
8Z0.1	13.84	23.68±0.65	9.41±0.66
8Z0.15	13.84	23.42±0.68	8.93±0.76

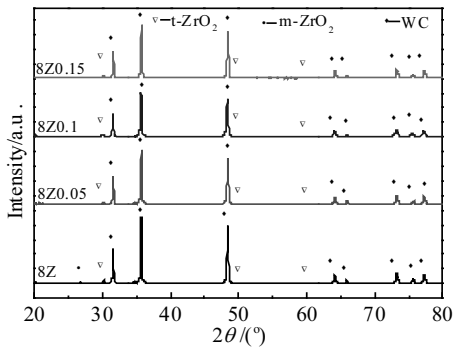

Fig.2 XRD patterns of composite specimens

Table 1 lists both the hardness and fracture toughness of WC-8wt%ZrO_2 and WC-8wt%ZrO_2 with the addition of UPBNNF composites. The 8Z0.05 specimen (hardness of 24.52±0.43 GPa; fracture toughness of 8.92±0.16 MPa·$m^{1/2}$) exhibits better hardness and fracture toughness compared to those of 8Z (hardness of 23.15±0.63 GPa; fracture toughness of 8.59±0.86 MPa·$m^{1/2}$), which increase by 5.9% and 3.8%, respectively. Fig.5 shows the crack path details of all composites. UPBNNF appears in the crack images of UPBNNF-containing specimens. In particular, single fibers can be observed between the broken parts of ZrO_2 in Fig.5b (Fig.5e is the magnified view of zone A in Fig.5b). There is a strong bonding between WC and ZrO_2. As the fraction of UPBNNF increases, both WC and ZrO_2 grains are coerced by agglomerates of fibers. Table 2 shows the calculated and tested Young's modulus of specimens[12]. 8Z0.5 specimens in two sets show abnormally high values (the highest value reaches to 692 GPa), which is close to the Young's modulus of pure WC (tested value, ~700 GPa), with a small change in density.

The variation in Young's modulus, which is the intrinsic property of materials determined by bonding of atoms[13], is the most remarkable phenomenon. The difficulty is that atoms deviate from inherent locations by external force resulting in the increase of Young's modulus. For composites, Young's modulus is a mass average value following the rule of mixtures, although there are several models of Young's modulus of the mixture[14]. A loose upper bound can be obtained using the Voigt formula:

$$E=\sum E_i V_i \quad (2)$$

where E_i and V_i denote Young's modulus and volume fraction of every phase, respectively. In this study, the value of cubic boron nitride is used for calculating the Young's modulus of the composites with UPBNNF. In fact, UPBNNF can be omitted from the calculations because of turbostratic structure with high porosity[15,16]. Moreover, several cases with restricted deviation are attributed to the contamination of material such as WC, which has a high Young's modulus[17,18]. Furthermore, there is no abnormity in the Young's modulus of WC-ZrO_2 composites tested by pulse-echo overlap ultrasonic technique in the research of Basu et al[7,8]. In addition, a variety of examination methods for bulks with different shapes show little difference on precision[19-21]. Meanwhile, it's also considered that new phases like ZrB_2 can be generated to improve the Young's modulus. However, the chemical kinetic condition is too strict to meet resulting in the fact that the Young's modulus of ZrB_2 is not high enough[22].

The difficulty of atoms deviating from inherent locations in the composites increases through the rise of external restriction when the Young's modulus increases. The materials can be impacted at a nanoscale (<50 nm)[23,24]. Firstly, the pore size of UPBNNF is quite small. It has a characteristic pore size of 2.7 nm according to the non-local density functional theory method[10]. Secondly, the grain can fill into the pore well. However, the average grain size is >100 nm for WC as a typical ceramic with the particle size of 200 nm[2]. So the WC phase has no possibility of the improvement of elastic property. Any phenomena of higher Young's modulus cannot be observed in WC-UPBNNF composites[25]. In fact, the ZrO_2 grain is well-known for its super plasticity[26]. Both the pore size and grain size can match during sintering. Then the ZrO_2 filler is restricted by the pore, which leads to an increase in the Young's modulus of ZrO_2. However, the match probability is lower because of agglomeration observed in the porous fibers.

Furthermore, the improvement of fracture toughness is related to the increase of Young's modulus. E/H in the formula of fracture toughness calculation is also an index to estimate the fracture toughness in a view of energy dissipation[27,28]. Fracture toughness is better when E/H rises. The biggest value of 8Z0.05 is up to 28.83, comparing with the value 24.30 of 8Z. According to classic fracture theory, it's also expected that the second phase possesses higher Young's modulus because of elevating energy consuming of fracture[29,30]. ZrO_2 combining UPBNNF with higher Young's modulus can meet the requirement. In a word, Young's modulus affects fracture toughness[28].

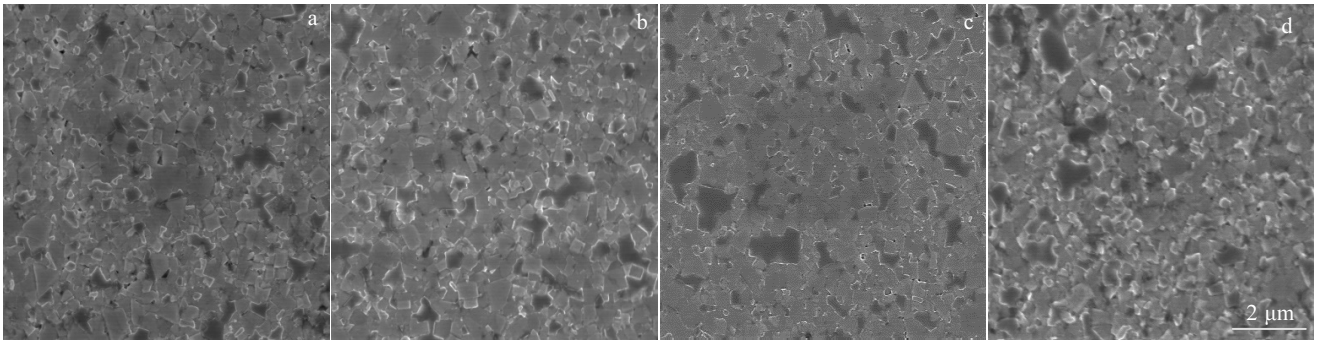

Fig.3 Typical SEM images of composite specimens: (a) 8Z, (b) 8Z0.05, (c) 8Z0.1, and (d) 8Z0.15

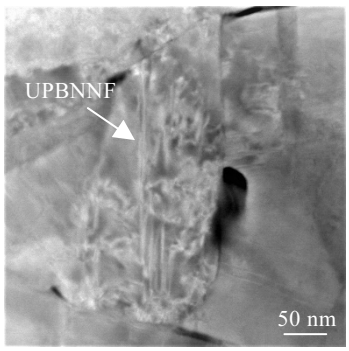

Fig.4 STEM image of UPBNNF in WC grains

Table 2 Tested and calculated Young's modulus of composite specimens (GPa)

Specimens	8Z	8Z0.05	8Z0.1	8Z0.15
Group 1	559	692	570	573
Group 2	544	624	570	550
Calculated value (Voigt)	575	577	578	579

Note: tested Young's modulus of cubic boron nitride (901 GPa) was used for calculations[12]

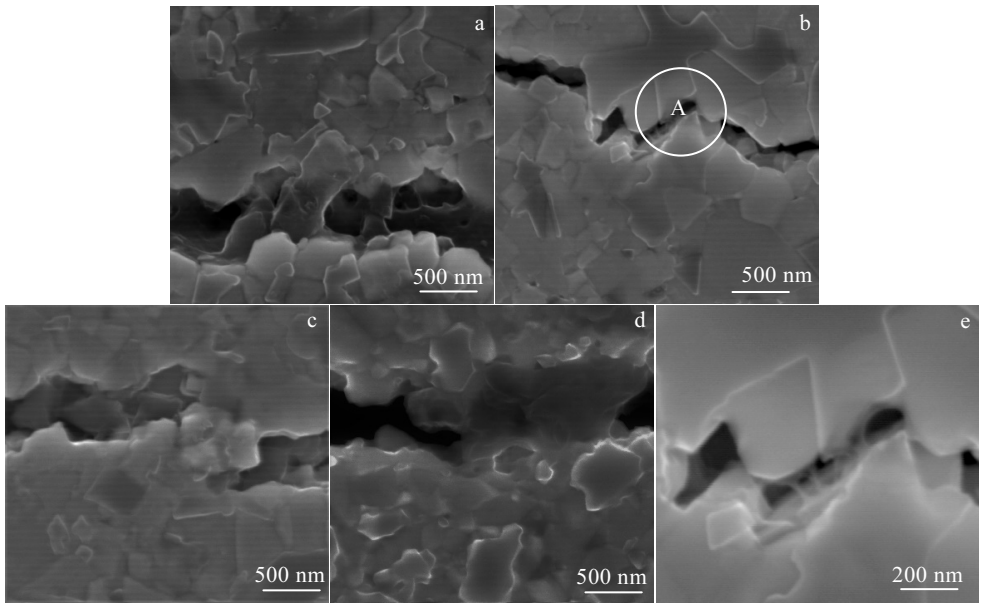

Fig.5 HRSEM images of crack path of different composite specimens: (a) 8Z, (b) 8Z0.05, (c) 8Z0.1, (d) 8Z0.15, and (e) zone A in Fig.5b

3 Conclusions

1) Compared with WC-8wt%ZrO_2 without the addition of UPBNNF (hardness of 23.15±0.63 GPa; fracture toughness of 8.59±0.86 MPa·$m^{1/2}$), the mean value of hardness and fracture toughness of WC-8wt%ZrO_2-0.05wt% UPBNNF increase by 5.9% and 3.8%, respectively.

2) WC-8wt%ZrO_2-0.05wt% UPBNNF shows a high Young's modulus (692 GPa), which is beyond the traditional rule of mixtures.

References

1 Cha S I, Hong S H. *Materials Science & Engineering A*[J], 2003, 356(1-2): 381

2 Poetschke J, Richter V, Holke R. *International Journal of Refractory Metal & Hard Materials*[J], 2012, 31: 218

3 García J, Ciprés V C, Blomqvist A *et al*. *International Journal of Refractory Metal & Hard Materials*[J], 2019, 80: 40

4 Hannink R H J, Kelly P M, Muddle B C. *Journal of the American Ceramic Society*[J], 2000, 83(3): 461

5 Tatarko P, Grasso S, Chlup Z *et al*. *Journal of the European Ceramic Society*[J], 2014, 34(7): 1829

6 Chen X, Luo L, Liu L *et al*. *Materials Science & Engineering A*[J], 2019, 740-741: 390

7 Basu B, Lee J H, Kim D Y. *Journal of the American Ceramic Society*[J], 2004, 87(2): 317

8 Basu B, Venkateswaran T, Sankar D. *Journal of the European Ceramic Society*[J], 2005, 25(9): 1603

9 Zheng D, Li X, Li Y *et al*. *Journal of Alloys & Compounds*[J], 2013, 572: 62

10 Lin J, Xu L, Huang Y *et al*. *RSC Advances*[J], 2016, 6(2): 1253

11 Niihara K, Morena R, Hasselman D P H. *Journal of Materials Science Letters*[J], 1982, 1(1): 13

12 Liu G, Kou Z, Yan X *et al*. *Applied Physics Letters*[J], 2015, 106(12): 121 901

13 Sherman D, Brandon D. *Advanced Engineering Materials*[J], 1999, 1(3-4): 161

14 Hsieh C L, Tuan W H. *Materials Science & Engineering A*[J], 2005, 393: 133
15 Pabst W, Gregorová E. *Journal of Materials Science*[J], 2004, 39(10): 3501
16 Frank E, Hermanutz F, Buchmeiser M R. *Macromolecular Materials & Engineering*[J], 2012, 297(6): 493
17 Fahrenholtz W G, Neuman E W, Brown-Shaklee H J *et al*. *Journal of the American Ceramic Society*[J], 2010, 93(11): 3580
18 Feng L, Fahrenholtz W G, Hilmas G E *et al*. *Journal of the American Ceramic Society*[J], 2019, 102(10): 5786
19 Koopman M, Chawla K K, Coffin C *et al*. *Advanced Engineering Materials*[J], 2002, 4(1-2): 37
20 Zhu S, Fahrenholtz W G, Hilmas G E *et al*. *Journal of the American Ceramic Society*[J], 2007, 90(11): 3660
21 Fahrenholtz W G, Neuman E W, Brown-Shaklee H J *et al*. *Journal of the American Ceramic Society*[J], 2010, 93(11): 3580
22 Yan C, Liu R, Zhang C *et al*. *Journal of the American Ceramic Society*[J], 2016, 99(1): 16
23 Gleiter H. *Progress in Materials Science*[J], 1989, 33(4): 223
24 Maglia F, Tredici I G, Anselmi-Tamburini U. *Journal of the European Ceramic Society*[J], 2013, 33(6): 1045
25 Li X, Cao T, Zhang M *et al*. *International Journal of Applied Ceramic Technology*[J], 2020, 17(3): 941
26 Okamoto T, Yasuda K, Shiota T. *Scripta Materialia*[J], 2011, 64(3): 253
27 Sebastiani M, Johanns K E, Herbert E G *et al*. *Current Opinion in Solid State & Materials Science*[J], 2015, 19(6): 324
28 Liu X, Wang H, Song X *et al*. *Transactions of Nonferrous Metals Society of China*[J], 2018, 28(5): 966
29 Marshall D B, Evans A G. *Journal of the American Ceramic Society*[J], 1985, 68(5): 225
30 Becher P F. *Journal of the American Ceramic Society*[J], 1991, 74(2): 255

超细氮化硼多孔纤维对 $WC-ZrO_2$ 复合材料力学性能的改善

曹 廷[1]，李小强[1]，李京懋[1]，黄 阳[2]，宋 涛[2]，屈盛官[1]，梁 良[1]
(1. 华南理工大学，广东 广州 510640)
(2. 河北工业大学，天津 300130)

摘 要：多孔纤维的研究传统上一般局限于催化和环境化学领域。而本研究将一种超细氮化硼多孔纤维被加入 WC-8%ZrO_2（质量分数）复合材料，以期改善其力学性能。结果表明，这种纤维的加入使得材料的杨氏模量、硬度和断裂韧性都得到了改善。然而，加入超细氮化硼多孔纤维样品的杨氏模量的提升并不遵循常用于评价陶瓷基材料杨氏模量的混合法则。个别添加了 0.05%超细氮化硼多孔纤维的样品的杨氏模量高达 692 GPa，已经接近纯 WC 材料的杨氏模量 700 GPa。这种现象可以通过基于 ZrO_2 的超塑性实现的纳米材料的小尺寸效应得到解释。

关键词：多孔纳米纤维；WC；ZrO_2；杨氏模量

作者简介：曹 廷，男，1983 年生，博士生，华南理工大学机械与汽车工程学院，广东 广州 510640，电话：020-87112111，E-mail: ctct_13@163.com